



**Showcasing research from Professor Nicolas Plumeré's laboratory, Faculty of Chemistry and Biochemistry, Ruhr-University Bochum, Germany.**

Reactivation of sulfide-protected [FeFe] hydrogenase in a redox-active hydrogel

[FeFe] hydrogenases are highly active hydrogen conversion catalysts, whose oxygen sensitivity prevents their widespread application. Here, an oxygen-stable inactive form was reactivated in a redox hydrogel enabling its practical use under air. Image designed and illustrated by Jo Richers.

**As featured in:**



See Alaa A. Oughli, James A. Birrell, Nicolas Plumeré *et al.*, *Chem. Commun.*, 2020, **56**, 9958.



Cite this: *Chem. Commun.*, 2020, 56, 9958

Received 1st May 2020,  
Accepted 23rd July 2020

DOI: 10.1039/d0cc03155k

rsc.li/chemcomm

## Reactivation of sulfide-protected [FeFe] hydrogenase in a redox-active hydrogel†

Alaa A. Oughli,<sup>a</sup> Steffen Hardt,<sup>a</sup> Olaf Rüdiger,<sup>b</sup> James A. Birrell<sup>b</sup> and Nicolas Plumeré<sup>a</sup>

[FeFe] hydrogenases are highly active hydrogen conversion catalysts but are notoriously sensitive to oxidative damage. Redox hydrogels have been used for protecting hydrogenases from both high potential inactivation and oxygen inactivation under turnover conditions. However, [FeFe] hydrogenase containing redox hydrogels must be fabricated under strict anoxic conditions. Sulfide coordination at the active center of the [FeFe] hydrogenase from *Desulfovibrio desulfuricans* protects this enzyme from oxygen in an inactive state, which can be reactivated upon reduction. Here, we show that this oxygen-stable inactive form of the hydrogenase can be reactivated in a redox hydrogel enabling practical use of this highly O<sub>2</sub> sensitive enzyme without the need for anoxic conditions.

Hydrogenases are metalloenzymes that catalyze the reversible conversion of H<sub>2</sub> into protons and electrons.<sup>1</sup> They have been studied extensively as promising candidates for energy conversion applications because of their high catalytic efficiencies.<sup>2</sup> However, hydrogenases suffer from oxidative deactivation pathways, which limit their use in devices.<sup>3</sup> In the past few years, protective redox-active matrices have been developed in order to tackle these limitations.<sup>4–6</sup> The redox active components of these matrices mediate electron transfer between the entrapped enzyme and the electrode surface, thus, providing a redox buffer that prevents inactivation induced by the high potentials imposed by the electrode.<sup>5,7</sup> Additionally, owing to the O<sub>2</sub>-reducing properties of the redox-active moieties bound to the matrix, O<sub>2</sub> is reduced in the outer layers of the film, maintaining anoxic conditions in the inner layers, where catalytic H<sub>2</sub> oxidation takes place.<sup>5,8</sup> Controlling the film thickness<sup>9</sup> enables optimization of the biocatalyst loading and life time,<sup>10</sup>

reaching time scales of weeks under turnover and constant exposure to oxygen.<sup>11</sup>

[FeFe] hydrogenases are considered to be the most active and reversible among the hydrogenase classes and, therefore, particularly relevant for biotechnological applications.<sup>12</sup> However, the high efficiency of [FeFe] hydrogenases comes with extreme oxygen sensitivity.<sup>13</sup> Thus, handling of the enzyme, including for catalytic hydrogel film preparation must be performed under strict anoxic conditions,<sup>4</sup> which is impractical, time consuming, and an impediment for upscaling the use of these catalysts. A simple chemical procedure has been reported for the protection of one of the most active [FeFe] hydrogenases, the enzyme from *Desulfovibrio desulfuricans* (*DdHydAB*).<sup>14</sup> This procedure involves oxidation of the enzyme in the presence of Na<sub>2</sub>S to produce an air-stable inactive state, named H<sub>inact</sub> (Scheme 1). The protected enzyme was stable under air for several days and could be reactivated under reducing conditions.

Here, we show that sulfide protected *DdHydAB* can be embedded in a redox hydrogel film, based on a low potential viologen as the redox mediator, under air, and then reactivated under hydrogen. Hydrogen spontaneously activates some of the enzymes from the catalytically inactive air-stable state H<sub>inact</sub> to the active oxidized O<sub>2</sub>-sensitive H<sub>ox</sub> state.<sup>15</sup> Those active enzymes then reduce the viologen moieties in the hydrogel,



**Scheme 1** Protection of *DdHydAB* with sulfide under oxidative conditions and its reactivation in a redox film under reductive conditions.

<sup>a</sup> Centre for Electrochemical Sciences—Molecular Nanostructures, Ruhr-Universität Bochum Universitätsstrasse 150, 44780 Bochum, Germany.

E-mail: nicolas.plumere@rub.de, alaa.alsheikhoughli@rub.de

<sup>b</sup> Max Planck Institute for Chemical Energy Conversion, Stiftstrasse 34–36, 45470 Mülheim an der Ruhr, Germany. E-mail: james.birrell@cec.mpg.de

† Electronic supplementary information (ESI) available. See DOI: 10.1039/d0cc03155k





which in turn transfers electrons to the rest of the protected enzyme causing them to activate rapidly (Scheme 1). Once activated, the enzyme delivers electrons from  $\text{H}_2$  oxidation to the viologen modified hydrogel film to block the incoming  $\text{O}_2$  and thus sustain its electrocatalytic activity in the presence of oxygen (Fig. 1A). Iodide ions added to the electrolyte catalyze the decomposition of reactive oxygen species (generated from the viologen catalyzed  $\text{O}_2$  reduction) to water preventing damage to the matrix, as reported previously.<sup>11</sup>

The efficiency of the protection/reactivation procedure was demonstrated *via* cyclic voltammetry experiments. Redox hydrogel films were prepared by drop-casting a mixture of *DdHydAB* and a 2,2'-viologen modified polyvinylalcohol backbone<sup>16</sup> (P1) (Scheme S1, ESI†) on a glassy carbon electrode. Electrodes were modified either with the sulfide protected enzyme<sup>14</sup> or with the unprotected enzyme (without sulfide treatment)<sup>17</sup> and left to dry under aerobic conditions for 16 h. Cyclic voltammograms of the electrodes modified with protected enzymes show catalytic hydrogen oxidation activity (Fig. 1B and Fig. S1, ESI†) with current densities of  $720 \pm 135 \mu\text{A cm}^{-2}$  (standard deviation of  $n = 5$  electrodes). Hence, the reactivation process was successful and the enzyme could sustain its catalytic activity despite exposure to  $\text{O}_2$  prior to reactivation. In contrast, when similar electrode preparation was performed using unprotected *DdHydAB*, redox signals only from the viologen of the redox-active polymer can be observed and no catalytic  $\text{H}_2$  oxidation activity was recorded (Fig. 1C). The same unprotected enzyme exhibited catalytic  $\text{H}_2$  oxidation activity in the redox-active film when the electrode was prepared and measured under anaerobic conditions (Fig. S2, ESI†). Therefore, the lack of catalytic activity in Fig. 1C can be attributed to  $\text{O}_2$  damage<sup>18</sup> of the unprotected enzyme during the aerobic preparation period.

Evidence for the reactivation mechanism can be obtained from experiments under various  $\text{H}_2$  concentrations. When cyclic voltammograms of electrodes modified with the sulfide protected enzyme are measured starting from a high potential in  $\text{H}_2$ -saturated buffer, the electrode immediately exhibits maximum catalytic current at the beginning of the scan, even before going to negative potentials (Fig. S3, ESI†). This is attributed to the spontaneous activation of the  $\text{H}_{\text{inact}}$  state by

$\text{H}_2$ . However, it was reported that the rates of reactivation are faster in the presence of a reducing agent (*e.g.* dithionite) or an electron mediator.<sup>15</sup> In the redox hydrogel matrix, the viologen moieties behave as electron mediators allowing rapid exchange of electrons between the enzymes. Insights on the timescale of the reactivation of the protected enzyme embedded in the redox polymer can be obtained from chronoamperometry experiments at low  $\text{H}_2$  concentrations and high potentials (Fig. S4, ESI†). The applied high potential under Ar ensures the oxidation of the redox polymer film. After addition of  $\text{H}_2$  (10%) to the Ar gas flow, the current does not significantly change initially. However, after a delay of  $85 \pm 4$  s (standard deviation for  $n = 5$  electrodes) the catalytic  $\text{H}_2$  oxidation current then increases rapidly. In contrast, when the same procedure is applied to the activated enzyme, a sharp increase of catalytic activity is observed instantly upon  $\text{H}_2$  addition indicating that the delay in the case of the protected enzyme is due to an initially slow progression of the reactivation process rather than equilibration of  $\text{H}_2$  in the electrolyte or in the polymer film. This behavior is attributed to an autocatalyzed reactivation process initiated by spontaneous activation of a small fraction of the enzyme by  $\text{H}_2$ . The initially activated fraction of the hydrogenase then catalyzes  $\text{H}_2$  oxidation and the resulting electrons are transferred to the viologen moieties, which rapidly activate the rest of the enzyme in the film.

To gain further insight on the reactivation process of the enzyme in the redox-active polymer in the absence of  $\text{H}_2$ , FTIR spectroelectrochemical measurement was performed on protected *DdHydAB* embedded in the film (Fig. 2 and Fig. S5, ESI†). FTIR assignments of the different states of the *DdHydAB* active site are well documented in the literature.<sup>14,17,19,20</sup> The film was formed on a gold mesh working electrode placed on top of a  $\text{CaF}_2$  window of a spectroelectrochemical cell based on a previously published design.<sup>21</sup> The cell was assembled under air and the applied potential was swept from positive to negative, equilibrating the potential for 30 minutes at each step. At high applied potentials (0 mV *vs.* SHE) the enzyme is mostly in the air-stable  $\text{H}_{\text{inact}}$  state (Fig. 2, green peaks). When applying more reducing potentials ( $-325$  mV *vs.* SHE) approaching the redox potential of the viologen ( $E_v = -440$  mV *vs.* SHE), the FTIR signals from the



**Fig. 1** Activation of sulfide-protected [FeFe] hydrogenase *DdHydAB* in a redox hydrogel. (A) Scheme illustrating the electron transfer routes in the redox-active film. The blue circles represent the viologen ( $\text{V}^{++}$ ) redox mediators. Cyclic voltammograms under Ar (blue trace) and  $\text{H}_2$  (black trace) of sulfide-protected *DdHydAB* (B) and standard *DdHydAB* (C) embedded in the redox polymer P1. Both electrodes were prepared on the lab bench under air. Conditions: Tris-citrate buffer (50 mM, pH 8.8) and KI (100 mM) as supporting electrolyte, room temperature, 2000 rpm,  $20 \text{ mV s}^{-1}$ .



**Fig. 2** FTIR spectroelectrochemistry of protected *DdHydAB* embedded in the viologen modified polymer P1 under air. FTIR spectra at selected applied potentials are shown to highlight the main states observed during the redox titration:  $H_{inact}$  (green),  $H_{trans}$  (orange),  $H_{ox}$  (red),  $H_{ox-CO}$  (gray),  $H_{red-CO}$  (purple).

one-electron reduced, but still inactive,  $H_{trans}$  state<sup>14</sup> (Fig. 2, orange peaks) become predominant. This is the first step in the enzyme reactivation in which the enzyme is still protected. The  $H_{trans}$  state is thought to retain the sulfur species bound to the active site. Going to more negative potentials ( $-425$  mV vs. SHE), near  $E_V$ , leads to the conversion of the  $H_{trans}$  state to the oxidized active state  $H_{ox}$  (Fig. 2, red peaks), with  $H_2S$  release from the enzyme, causing deprotection and activation of catalysis. In parallel to  $H_{ox}$  formation, signals from the CO-inhibited state  $H_{ox-CO}$  (Fig. 2, gray peaks) are visible. This state is formed when CO coordinates to the active site of a deprotected hydrogenase. The presence of the  $H_{ox-CO}$  state suggests that CO has been released from damage of a fraction of the enzyme.<sup>20</sup> Within the confined volume of the spectroelectrochemical cell CO cannot escape from the inhibited enzyme. However, when the enzyme is under turnover conditions in the presence of  $H_2$  in an open electrochemical cell, this CO is released, giving rise to the large catalytic currents observed in Fig. 1B.

The reductive deprotection and release of the sulfide ligand from  $H_{inact}$  reactivates the enzyme's ability to oxidize hydrogen but also its sensitivity toward oxygen. This is illustrated in a chronoamperometry experiment of protected *DdHydAB* after reactivation. When the enzyme is measured in the absence of the hydrogel film as a protection matrix, by simply adsorbing the protein on a graphite electrode surface, catalytic  $H_2$  oxidation activity is irreversibly lost upon the addition of 5%  $O_2$  to the gas feed (Fig. 3, red trace). The negative current observed under 5%  $O_2$  is due to direct  $O_2$  reduction at the electrode surface. In contrast, when the protected *DdHydAB* was embedded in the redox hydrogel, the addition of  $O_2$  led only to a slight decrease in the current, which was fully recovered once  $O_2$  was removed from the gas feed (Fig. 3, black trace). This decrease of the current in presence of  $O_2$  is due to the decrease of the electron flux toward the electrode as some of the electrons generated from the hydrogenase catalyzed  $H_2$  oxidation are diverted toward the outer layer of the film to reduce  $O_2$  preventing it from reaching the enzyme (Fig. 1A), as reported previously.<sup>4,5,8</sup>

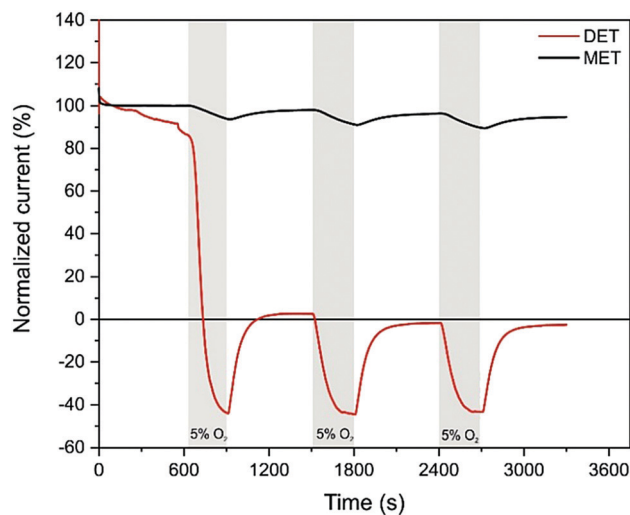


**Fig. 3** Oxygen tolerance under turnover conditions. Chronoamperometry experiments of a glassy carbon electrode modified with a mixture of sulfide-protected *DdHydAB* and the viologen modified polymer P1 (black trace), and a pyrolytic graphite electrode modified with sulfide-protected *DdHydAB* in a DET regime (red trace). The concentration of  $H_2$  was kept constant at 95% and Ar was used as an inert gas to complete the mixture. The shaded area indicates addition of 5%  $O_2$  to the gas feed for 300 s. Chronoamperometry was recorded in Tris-citrate buffer (50 mM, pH 8.8) with KI (100 mM) as supporting electrolyte at  $-201$  mV vs. SHE and 2000 rpm. The DET experiment was performed in an anaerobic glovebox at room temperature.

In conclusion, we have demonstrated that the oxygen-stable sulfide-protected form of *DdHydAB* can be incorporated into redox-active hydrogel films, under air, and reactivated under reductive conditions giving a catalytically active electrode. The source of electrons for reactivation can either be the electrode poised at reducing potentials or  $H_2$ . The sulfide protection allowed aerobic preparation of the biocatalytic films, which was not possible with the unprotected enzyme. After sulfide deprotection, the enzyme is intrinsically  $O_2$  sensitive but its  $O_2$  induced inactivation is prevented in the redox-active hydrogel matrix owing to the local anaerobic conditions established under turnover conditions for  $H_2$  oxidation. This combination of matrix-induced reactivation and matrix-induced protection simplifies the integration of highly  $O_2$  sensitive catalysts in devices by circumventing the need for anaerobic conditions for both the electrode preparation and for electrocatalytic applications.

This approach may also be advantageous for applying synthetic molecular catalysts that are prone to  $O_2$  damage.<sup>22</sup> Some recent reports have demonstrated that reductive treatment can reactivate the  $O_2$  inactivated states of some artificial systems or that proper design of the coordination sphere can limit the  $O_2$  damage.<sup>23</sup> While these previous efforts aimed at robust catalysts for  $H^+/H_2$  conversion under  $O_2$ , we believe that our demonstration of the reductive reactivation and operation of a highly  $O_2$  sensitive enzyme in redox-active matrices opens the possibility to apply synthetic catalysts that show  $O_2$  stable inactive and  $O_2$  sensitive active states in the same way.

N. P., A. A. O and S. H. acknowledge financial support by the ERC starting grant 715900, by the ANR-DFG project SHIELDS



(PL 746/2-1) and by RESOLV, funded by the Deutsche Forschungsgemeinschaft (DFG, German Research Foundation) under Germany's Excellence Strategy – EXC-2033 – Projektnummer 390677874. J. A. B. and O. R. are supported by the Max Planck Society and J. A. B. acknowledges funding from the Deutsche Forschungsgemeinschaft (DFG) Priority Programme “Iron-Sulfur for Life: Cooperative Function of Iron-Sulfur Centers in Assembly, Biosynthesis, Catalysis and Disease” (SPP 1927) Project BI 2198/1-1. The authors thank L. Castaneda-Losada, J. Jaenecke, F. Hiege, L. Dubbert, C. Spula, L. Engelhard and C. Kim for useful discussions and preliminary experiments, Nina Breuer for the preparation of the hydrogenase. Open Access funding provided by the Max Planck Society.

## Conflicts of interest

There are no conflicts to declare.

## Notes and references

- 1 J. W. Peters, G. J. Schut, E. S. Boyd, D. W. Mulder, E. M. Shepard, J. B. Broderick, P. W. King and M. W. W. Adams, *Biochim. Biophys. Acta*, 2015, **1853**, 1350–1369.
- 2 W. Lubitz, H. Ogata, O. Rüdiger and E. Reijerse, *Chem. Rev.*, 2014, **114**, 4081–4148.
- 3 J. A. Cracknell, K. A. Vincent and F. A. Armstrong, *Chem. Rev.*, 2008, **108**, 2439–2461.
- 4 A. A. Oughli, F. Conzuelo, M. Winkler, T. Happe, W. Lubitz, W. Schuhmann, O. Rüdiger and N. Plumeré, *Angew. Chem., Int. Ed.*, 2015, **54**, 12329–12333.
- 5 N. Plumeré, O. Rüdiger, A. A. Oughli, R. Williams, J. Vivekananthan, S. Pöller, W. Schuhmann and W. Lubitz, *Nat. Chem.*, 2014, **6**, 822–827.
- 6 K. Sakai, Y. Kitazumi, O. Shirai, K. Takagi and K. Kano, *ACS Catal.*, 2017, **7**, 5668–5673.
- 7 (a) L. H. Eng, M. Elmgren, P. Komlos, M. Nordling, S.-E. Lindquist and H. Y. Neujahr, *J. Phys. Chem.*, 1994, **98**, 7068–7072; (b) S. V. Morozov, E. E. Karyakina, N. A. Zorin, S. D. Varfolomeyev, S. Cosnier and A. A. Karyakin, *Bioelectrochemistry*, 2002, **55**, 169–171.
- 8 V. Fourmond, S. Stapf, H. Li, D. Buesen, J. Birrell, O. Rüdiger, W. Lubitz, W. Schuhmann, N. Plumeré and C. Léger, *J. Am. Chem. Soc.*, 2015, **137**, 5494–5505.
- 9 (a) H. Li, D. Buesen, R. Williams, J. Henig, S. Stapf, K. Mukherjee, E. Freier, W. Lubitz, M. Winkler, T. Happe and N. Plumeré, *Chem. Sci.*, 2018, **9**, 7596–7605; (b) D. Buesen, H. Li and N. Plumeré, *Chem. Sci.*, 2020, **11**, 937–946.
- 10 H. Li, D. Buesen, S. Dementin, C. Léger, V. Fourmond and N. Plumeré, *J. Am. Chem. Soc.*, 2019, **141**, 16734–16742.
- 11 H. Li, U. Münchberg, A. A. Oughli, D. Buesen, W. Lubitz, E. Freier and N. Plumeré, *Nat. Commun.*, 2020, **11**, 920.
- 12 B. R. Glick, W. G. Martin and S. M. Martin, *Can. J. Microbiol.*, 1980, **26**, 1214–1223.
- 13 M. W. Adams, *Biochim. Biophys. Acta*, 1990, **1020**, 115–145.
- 14 P. Rodríguez-Maciá, E. J. Reijerse, M. van Gastel, S. DeBeer, W. Lubitz, O. Rüdiger and J. A. Birrell, *J. Am. Chem. Soc.*, 2018, **140**, 9346–9350.
- 15 E. C. Hatchikian, N. Forget, V. M. Fernandez, R. Williams and R. Cammack, *Eur. J. Biochem.*, 1992, **209**, 357–365.
- 16 S. Hardt, S. Stapf, J. A. Birrell, O. Rüdiger, V. Fourmond, C. Léger and N. Plumeré, *Reversible H<sub>2</sub> oxidation and evolution by hydrogenase embedded in a redox polymer film*, submitted March 2020.
- 17 J. A. Birrell, K. Wrede, K. Pawlak, P. Rodríguez-Maciá, O. Rüdiger, E. J. Reijerse and W. Lubitz, *Isr. J. Chem.*, 2016, **56**, 852–863.
- 18 A. Kubas, C. Orain, D. de Sancho, L. Saujet, M. Sensi, C. Gauquelin, I. Meynial-Salles, P. Soucaille, H. Bottin, C. Baffert, V. Fourmond, R. B. Best, J. Blumberger and C. Léger, *Nat. Chem.*, 2017, **9**, 88–95.
- 19 P. Rodríguez-Maciá, J. A. Birrell, W. Lubitz and O. Rüdiger, *Chem-PlusChem*, 2017, **82**, 540–545.
- 20 S. P. J. Albracht, W. Roseboom and E. C. Hatchikian, *J. Biol. Inorg. Chem.*, 2006, **11**, 88–101.
- 21 D. Moss, E. Navedryk, J. Breton and W. Mantele, *Eur. J. Biochem.*, 1990, **187**, 565–572.
- 22 (a) A. Dutta, J. A. Roberts and W. J. Shaw, *Angew. Chem.*, 2014, **53**, 6487–6491; (b) P. Rodríguez-Maciá, A. Dutta, W. Lubitz, W. J. Shaw and O. Rüdiger, *Angew. Chem., Int. Ed.*, 2015, **54**, 12303–12307.
- 23 (a) X. Yang, L. C. Elrod, T. Le, V. S. Vega, H. Naumann, Y. Rezenom, J. H. Reibenspies, M. B. Hall and M. Y. Darensbourg, *J. Am. Chem. Soc.*, 2019, **141**, 15338–15347; (b) X. Yang, L. C. Elrod, J. H. Reibenspies, M. B. Hall and M. Y. Darensbourg, *Chem. Sci.*, 2019, **10**, 1368–1373.

